J|A|C|S COMMUNICATIONS

Published on Web 11/24/2009

Complete Conversion of Hydrous Hydrazine to Hydrogen at Room Temperature for Chemical Hydrogen Storage

Sanjay Kumar Singh and Qiang Xu*

National Institute of Advanced Industrial Science and Technology (AIST), Ikeda, Osaka 563-8577, Japan

Received September 21, 2009; E-mail: q.xu@aist.go.jp

Development of safe and efficient hydrogen storage materials remains one of the most difficult challenges on the way to a hydrogen energy based economy. Even after several decades of exploration, no single material investigated to date meets all the necessary transportation requirements, such as volumetric and gravimetric hydrogen capacities, handling pressure and temperature, recycling of byproduct, and so on.[1,2] Its solution requires innovative breakthroughs coming from scientific and technological research that looks beyond the storage materials currently known. Anhydrous hydrazine, H_2NNH_2, is a liquid at room temperature and has a hydrogen content as high as 12.5 wt %. Recent studies, mostly on the reactions of hydrazine highly diluted in inert gases such as argon, have shown that hydrazine can be decomposed in two ways: complete decomposition, $H_2NNH_2 \rightarrow N_2(g) + 2H_2(g)$ (1), and the incomplete decomposition, $3H_2NNH_2 \rightarrow 4NH_3 + N_2(g)$ (2); the reaction pathways depend on the catalyst used and the reaction conditions.[3,4] However, anhydrous hydrazine is explosive to a metal catalyst, making it difficult to apply safely.[5] Hydrous hydrazine, such as hydrazine monohydrate, $H_2NNH_2 \cdot H_2O$, a liquid at room temperature having a hydrogen content as high as 7.9 wt % and being safe in handling,[5] could be a potential hydrogen storage material that has the distinguished advantages of easy recharging as well as the only production of nitrogen (which does not need recycling) besides hydrogen by complete decomposition. Encouraged by the high potential of hydrous hydrazine, we have recently examined a number of transition metal catalysts for its decomposition to generate hydrogen at room temperature and found that Rh nanoparticles (NPs) exhibit the highest catalytic activity, while the maximum hydrogen selectivity was limited to 43.8%.[6] An obvious question arises: is it possible to achieve 100% selectivity for hydrogen by the room-temperature decomposition of hydrous hydrazine? Here, we report that the synergic effect of Rh and Ni in Rh−Ni alloy nanoparticles drastically enhances the hydrogen selectivity of our recently reported Rh NPs in the decomposition of hydrous hydrazine, which achieves 100% at Rh/Ni = 4:1.

The bimetallic Rh−Ni nanocatalysts were generated as a black suspension using a surfactant aided coreduction process by adding an aqueous solution of sodium borohydride, as a reducing agent, to an aqueous solution of rhodium(III) chloride and nickel(II) chloride in the presence of hexadecyltrimethyl ammonium bromide (CTAB). The resulted Rh_xNi_y (x = 1, 3, 4, 8, 16, 64 and y = 1, 4, 8, 16) nanocatalysts with various compositions of Rh and Ni are designated as $Rh_{64}Ni$, $Rh_{16}Ni$, Rh_8Ni, Rh_4Ni, Rh_3Ni, RhNi, $RhNi_4$, $RhNi_8$, and $RhNi_{16}$. After the absence of gas evolution from the solution was verified, hydrazine decomposition reaction was initiated by the introduction of hydrazine monohydrate into the reaction flask, resulting in the gas release, which was measured volumetrically.[7]

We have investigated the catalytic activities of Rh_xNi_y (Rh/Ni = 1:16−64:1) nanocatalysts to hydrous hydrazine decomposition reaction with the Rh/N_2H_4 molar ratio (1:10) kept unchanged and found that the selectivity to hydrogen strongly depends on the Rh/Ni ratio (Figure S1).[7] Surprisingly, despite nickel itself being inactive to this reaction, the presence of nickel drastically enhances the hydrogen selectivity which shows a maximum of 100% at Rh/Ni = 4:1 (Figure 1), indicating that hydrous hydrazine can be completely converted to hydrogen and nitrogen at room temperature. For Rh_4Ni, a release of 3.0 equiv of gases was observed in 160 min (Figure 1), which were identified by mass spectrometry to be hydrogen and nitrogen with a H_2/N_2 ratio of 2.0 (Figure S2),[7] in agreement with the volumetric observations. It is found that the $n(H_2+N_2)/n(N_2H_4)$ ratio of 3.0 remains unchanged with the increase in N_2H_4 concentration from 0.5 to 5.0 M keeping Rh/N_2H_4 = 1:10 (Figure S3),[7] or with the decrease in the Rh/N_2H_4 ratio from 1/10 to 1/100 keeping the N_2H_4 concentration at 0.5 M (Figure S4), indicating that the N_2H_4 concentration and the Rh/N_2H_4 ratio do not influence the hydrogen selectivity. It should be noted that no ^{15}N NMR signal was observed for ammonia after the decomposition of hydrazine (Figure S5),[7] confirming the complete conversion of hydrazine to hydrogen and nitrogen. Moreover, we have also examined the catalytic activities of the Rh_4M (M = Fe, Co and Cu) nanocatalysts and found that the addition of these metals (Fe, Co and Cu) to Rh shows negative effects on the hydrogen selectivity, in contrast with the drastically positive effect by the addition of Ni (Figure S6).[7]

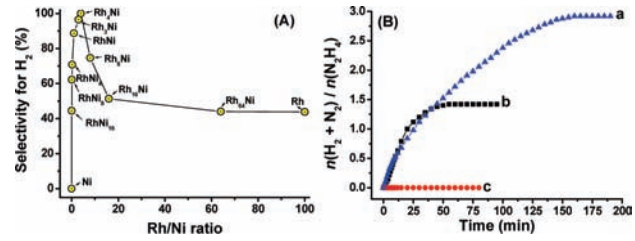

Figure 1. (A) Selectivity for hydrogen generation from hydrous hydrazine (0.5 M) catalyzed by Rh_xNi_y (x = 0−64; y = 0−16). with Rh/N_2H_4 = 1:10 at room temperature. (B). Time course plots for decomposition of hydrous hydrazine (0.5 M) catalyzed by (a) Rh_4Ni, (b) Rh (Rh/N_2H_4 = 1:10), and (c) Ni (Ni/N_2H_4 = 1:10) nanocatalysts at room temperature.

To identify the reason of the drastic enhancement by the addition of Ni to Rh, the catalytic activity of physically mixed Rh NPs and Ni NPs, which were separately prepared using a similar procedure, with a molar ratio of Rh/Ni = 4:1 was examined for the decomposition reaction of hydrous hydrazine. It was found that the physical mixing of Ni NPs, which are inactive to this reaction, to Rh NPs does not give significant effects to the hydrogen selectivity (Figure S7).[7] Therefore, the presence of Rh and Ni in the same material is a prerequisite for enhancing the hydrogen selectivity of the Rh nanocatalyst.

The morphology of Rh_4Ni, the most selective catalyst for the complete decomposition of hydrous hydrazine, has been character-

10.1021/ja908037t

ized by scanning electron microscopy (SEM, Figure S8)[7] and transmission electron microscopy (TEM, Figure 2). The typical TEM image (Figure 2a) reveals that nearly monodispersed Rh_4Ni NPs with an average particle size of ~3 nm are obtained. The high resolution TEM (HRTEM) image and the corresponding selected area energy dispersion (SAED) pattern indicate that the Rh_4Ni NPs are crystalline (Figure 2b). The intense high-angle annular dark-field scanning TEM (HAADF-STEM) image of the Rh_4Ni NPs along with the energy dispersion X-ray spectroscopic (EDS) analysis (Figure 2c) indicates a uniform bimetallic Rh−Ni nanocatalyst, in accord with the observation that the coreduced Rh_4Ni nanocatalyst shows enhanced hydrogen selectivity while the physically mixed Rh−Ni catalyst does not enhance the hydrogen selectivity in the decomposition of hydrous hydrazine. X-ray diffraction (XRD) was used to identify the crystalline structures of the prepared Rh−Ni nanocatalysts. The XRD pattern of Rh_4Ni shows that the peaks can be referenced to a face-centered cubic (FCC) unit cell with lattice constant $a = 3.828$ Å (Figure 2d). The 2θ values of 41.09°, 46.65°, 69.50°, and 85.35° can be indexed to diffractions of (111), (200), (220), and (311) planes, respectively (PDF #05-0685). Similar XRD profiles have also been observed for Rh_xNi_y ($x = 3-64$; $y = 1$), the nanocatalysts that have relatively high Rh contents (Figure S9).[7] For the nanocatalyst with high Ni contents, Rh_xNi_y ($x = 1$; $y = 8$, 16), XRD profiles similar to that of Ni ($a = 3.535$ Å) have been observed, whereas $RhNi_4$ shows an intermediate pattern between those of Rh and Ni (Figure S9).[7] In addition, the nitrogen adsorption−desorption isotherms (Figure S10) of the Rh_4Ni nanocatalyst revealed that the Brunauer−Emmett−Teller (BET) surface area is 55.6 $m^2\ g^{-1}$, comparable to that of Rh NPs.[6,7]

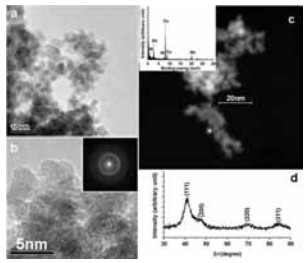

Figure 2. (a) TEM image, (b) high-resolution TEM (HRTEM) image (inset: the corresponding SAED pattern), (c) HAADF-STEM image with the corresponding (assigned as *) EDS spectrum (Cu signals in EDS are from Cu grids), and (d) XRD profile of Rh_4Ni nanocatalyst.

To understand the states of Rh and Ni that coexist in the Rh_4Ni nanocatalyst, X-ray photoelectron spectroscopic (XPS) measurements were carried out, which revealed that the Rh_4Ni nanocatalyst is composed of Rh^0 and Ni^0 (Figure S11).[7] A thin oxidized cover formed during the exposure of the sample to air, with binding energies for Rh $3d_{5/2}$ and Rh $3d_{3/2}$ at 308.2 and 312.9 eV, respectively, and binding energies for Ni $2p_{3/2}$ and Ni $2p_{1/2}$ at 857.2 and 874.4 eV, respectively,[8] which was readily removed by Ar sputtering for only 2 min. The observed Rh $3d_{5/2}$ and Rh $3d_{3/2}$ binding energies at 307.2 and 311.9 eV correspond to Rh^0, and the Ni $2p_{3/2}$ and Ni $2p_{1/2}$ binding energies at 852.9 and 870.2 eV correspond to Ni^0.[8] No change in the Rh/Ni ratio was observed with further Ar sputtering up to 174 min, indicating the homogeneity of the composition of Rh_4Ni nanocatalyst, in accord with the TEM and EDS observations.

Catalyst modification by introducing a second component or changing the morphology can substantially control the performance of catalyst.[9−11] Considering that Ni itself is inactive to the catalytic decomposition of hydrous hydrazine,[4] the synergistic effect of Rh and Ni that gives rise to the drastic enhancement of the hydrogen selectivity is surprising. It is reasonable to understand that the alloying of Rh and Ni leads to a modification of the catalyst surface[9,10] and tunes the interactions of Rh with the N−N and N−H bonds as well as the stability of reaction intermediates on the catalyst surface.[4] Consequently, the reaction prefers pathway (1) to pathway (2), resulting in a complete conversion of hydrazine to hydrogen and nitrogen.

In conclusion, we have demonstrated that alloying of Rh and Ni in the bimetallic Rh_4Ni nanocatalyst makes it possible to achieve 100% conversion of hydrous hydrazine to hydrogen at room temperature, bringing hydrous hydrazine as a highly promising material for hydrogen storage. To meet practical applications, further work is needed for developing low-cost high-performance catalysts.

Acknowledgment. We acknowledge the reviewers for their valuable suggestions and JSPS and AIST for financial support. S.K.S. thanks JSPS for a postdoctoral fellowship. We are grateful to T. Umegaki, AIST, for his generous help in conducting XPS measurements.

Supporting Information Available: Details for the Rh−Ni nanocatalysts preparation and characterization by powder XRD, STEM, TEM and XPS, and the catalytic hydrazine decomposition experiments. This material is available free of charge via the Internet at http://pubs.acs.org.

References

(1) (a) Graetz, J. *Chem. Soc. Rev.* **2009**, *38*, 73–82. (b) Hamilton, C. W.; Baker, R. T.; Staubitz, A.; Manners, I. *Chem. Soc. Rev.* **2009**, *38*, 279–293. (c) Xiong, Z.; Yong, C. K.; Wu, G.; Chen, P.; Shaw, W.; Karkamkar, A.; Autrey, T.; Jones, M. O.; Johnson, S. R.; Edwards, P. P.; David, W. I. F. *Nat. Mater.* **2008**, *7*, 138–141. (d) Chandra, M.; Xu, Q. *J. Power Sources* **2006**, *156*, 190–194. (e) Xu, Q.; Chandra, M. *J. Power Sources* **2006**, *163*, 364–370. (f) Gutowska, A.; Li, L.; Shin, Y.; Wang, C. M.; Li, X. S.; Linehan, J. C.; Smith, R. S.; Kay, B. D.; Schmid, B.; Shaw, W.; Gutowski, M.; Autrey, T. *Angew. Chem.* **2005**, *44*, 3578–3582. (g) Chen, P.; Xiong, Z.; Luo, J.; Lin, J.; Tan, K. L. *Nature* **2002**, *420*, 302–304. (h) Schlapbach, L.; Züttel, A. *Nature* **2001**, *414*, 353–358.

(2) U. S. DOE, "Hydrogen, Fuel Cells & Infrastructure Technologies Program Multi-Year Research, Development, and Demonstration Plan, Hydrogen Storage Technical Plan, 2007", http://www1.eere.energy.gov/hydrogenandfuelcells/mypp/.

(3) (a) Gu, H.; Ran, R.; Zhou, W.; Shao, Z.; Jin, W.; Xu, N.; Ahn, J. *J. Power Sources* **2008**, *177*, 323–329. (b) Cho, S. J.; Lee, J.; Lee, Y. S.; Kim, D. P. *Catal. Lett.* **2006**, *109*, 181–187. (c) Zheng, M.; Cheng, R.; Chen, X.; Li, N.; Li, L.; Wang, X.; Zhang, T. *Int. J. Hydrogen Energy* **2005**, *30*, 1081–1089. (d) Chen, X.; Zhang, T.; Zheng, M.; Wu, Z.; Wu, W.; Li, C. *J. Catal.* **2004**, *224*, 473–478. (e) Armstrong, W. E.; Ryland, L. B.; Voge, H. H. *US Patent* **1978**, *4*, 124–538.

(4) (a) Santos, J. B. O.; Valença, G. P.; Rodrigues, J. A. J. *J. Catal.* **2002**, *210*, 1–6. (b) Prasad, J.; Gland, J. L. *Langmuir* **1991**, *7*, 722–726.

(5) Schmidt, E. W. *Hydrazine and its Derivatives: Preparation, Properties, Applications*, 2nd ed.; John Wiley & Sons: New York, 1984.

(6) Singh, S. K.; Zhang, X.-B.; Xu, Q. *J. Am. Chem. Soc.* **2009**, *131*, 9894–9895.

(7) See Supporting Information.

(8) Moulder, J. F.; Chastain, J.; King, R. C. *Handbook of X-ray Photoelectron Spectroscopy: A Reference Book of Standard Spectra for Identification and Interpretation of XPS Data*; Physical Electronics: Eden Prairie, MN, 1995.

(9) Ferrando, R.; Jellinek, J.; Johnston, R. L. *Chem. Rev.* **2008**, *108*, 845–910.

(10) Basile, F.; Fornasari, G.; Trifirò, F.; Vaccari, A. *Catal. Today* **2002**, *77*, 215–223.

(11) (a) Lim, B.; Jiang, M.; Camargo, P. H. C.; Cho, E. C.; Tao, J.; Lu, X.; Zhu, Y.; Xia, Y. *Science* **2009**, *324*, 1302–1305. (b) Zhang, X.-B.; Yan, J.-M.; Han, S.; Shioyama, H.; Xu, Q. *J. Am. Chem. Soc.* **2009**, *131*, 2778–2779. (c) Xie, X.; Li, Y.; Liu, Z.-Q.; Haruta, M.; Shen, W. *Nature* **2009**, *458*, 746–749. (d) Yan, J.-M.; Zhang, X.-B.; Han, S.; Shioyama, H.; Xu, Q. *Angew. Chem., Int. Ed.* **2008**, *47*, 2287–2289. (e) Heemeier, M.; Carlsson, A. F.; Naschitzki, M.; Schmal, M.; Bäumer, M.; Freund, H.-J. *Angew. Chem., Int. Ed.* **2002**, *41*, 4073–4076.

JA908037T